MR Imaging of Normal Perivascular Space Expansion at Midbrain

Naokatsu Saeki, Motoki Sato, Motoo Kubota, Yoshio Uchino, Hisayuki Murai, Yuichiro Nagai, Hiroshi Ishikura, Seitaro Nomura, Iichiro Matsuura and Akira Yamaura

AJNR Am J Neuroradiol 2005, 26 (3) 566-571
http://www.ajnr.org/content/26/3/566

AJNR Am J Neuroradiol 26:566–571, March 2005

MR Imaging of Normal Perivascular Space Expansion at Midbrain

Naokatsu Saeki, Motoki Sato, Motoo Kubota, Yoshio Uchino, Hisayuki Murai, Yuichiro Nagai, Hiroshi Ishikura, Seitaro Nomura, Iichiro Matsuura, and Akira Yamaura

BACKGROUND AND PURPOSE: **A previous investigation of the MR imaging findings in the midbrain reported expanded perivascular (PV) spaces in only the ponto-mesencepalic junction (PMJ) in 20% of healthy subjects, whereas pathologically expanding PV spaces have been reported at the mesencephalo-diencephalic junction (MDJ) as multi-lobulated, cystic lesions with signal intensity compatible with that of CSF that cause aqueductal stenosis. To clarify the anatomical distinctions between normally expanded and pathologically expanding PV spaces, we defined their distribution in the normal midbrain by using high-spatial-resolution MR imaging.**

METHODS: **Heavily T2-weighted MR imaging was performed in 115 adult subjects with neurologic complaints without cerebral disease. Histologic studies were performed from two normal midbrain blocks.**

RESULTS: **Expanded PV spaces were visible at the PMJ in 87% of subjects and at the MDJ in 63% of subjects. On axial images, ovoid or linear lesions with signal intensity compatible to CSF were present behind the cerebral peduncle at both the PMJ and MDJ. These areas varied from less than 1 mm to 5 mm (maximum diameter on coronal sections). Histologic studies confirmed the distribution of expanded PV spaces, as noted on MR images.**

CONCLUSION: **This study, by using high-spatial-resolution MR imaging, revealed that expanded PV spaces were visible at the PMJ and MDJ. Our finding of expanded PV spaces normally present at the MDJ may be related to pathologically expanding PV spaces, which should be kept in mind as a differential diagnosis for intraparenchymal cystic lesions in the midbrain with signal intensity compatible to CSF.**

The advent of high-spatial-resolution MR imaging makes it possible to observe expanded perivascular (PV) spaces in the brain. Clinically, these spaces are noteworthy as a differential diagnosis for lacunar infarcts (1–5). They are commonly found in the following locations: the lower third of the basal ganglia adjacent to the anterior commissure, the corona radiata and centrum semiovale, the hippocampus, the insula, and the midbrain (1–6). MR imaging observations of PV spaces in the midbrain of normal subjects were first reported by Elster and Richardson (2) in 1991. They reported PV spaces in 20% of healthy subjects at the ponto-mesencephalic junction (PMJ) but found no clinical correlate to these findings. Recently, pathologic studies from autopsy specimens (7) and MR imaging data (8–13) from several cases with aqueductal stenosis caused by multilobular CSF-filled expanding spaces at the mesencephalo-diencephalic junction (MDJ) have reported large cavities with a similar distribution to asymptomatic expanded PV spaces in the midbrain (Fig 1). Therefore, it is hypothesized that normal PV spaces undergoing expansion may contribute to mass effect (8–10). However, since symptomatic cases had lesions at the MDJ (Fig 1) (12), while normal PV spaces are located at the PMJ, further neuroanatomical studies are needed to establish the relationship between normal and pathologically expanded PV spaces.

T2-weighted MR imaging is known to detail fine structures in and around the CSF spaces and is considered a sensitive method for depicting PV spaces (14). To clarify the anatomical distinctions between normally expanded and pathologically expanding PV spaces, we defined their distribution in the normal midbrain by using high-spatial-resolution MR imaging.

Received August 19, 2003; accepted after revision January 5, 2004.

From the Departments of Neurological Surgery and Pathology, Chiba University Graduate School of Medicine.

Address reprint requests to Naokatsu Saeki, Department of Neurological Surgery, Chiba University Graduate School of Medicine, Inohana 1-8-1, Chuo-ku, Chiba City, Chiba 260-8670, Japan.

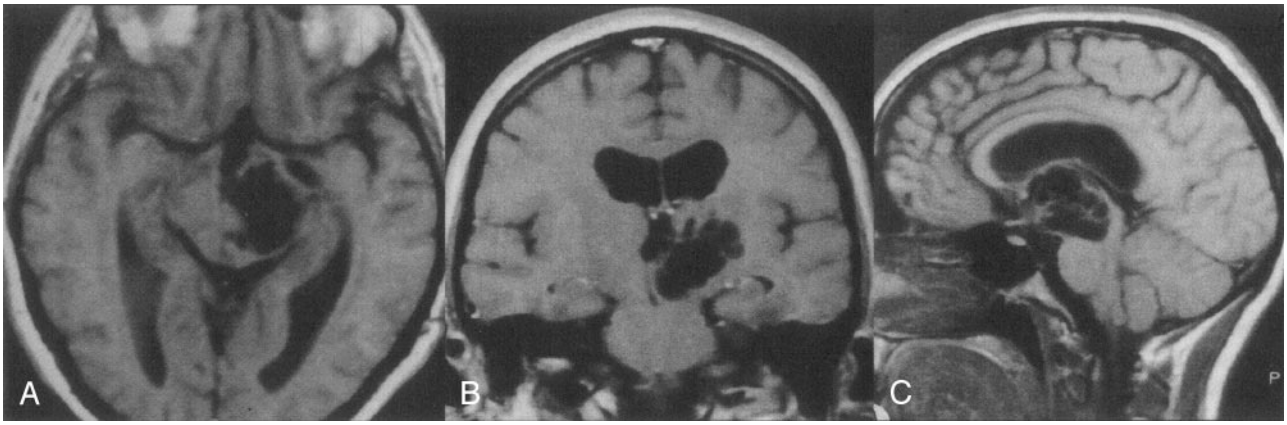

FIG 1. MR images obtained in a 32-year-old woman who presented with headache and progressive right hemiparesis; MR images revealed multilobular CSF-filled expanding spaces at the MDJ and ventricular dilatation. She underwent endoscopic fenestration of the cyst wall and became free of the neurologic deficits. (Reproduced with permission from reference 12.)

T1-weighted axial (A), coronal (B), and sagittal (C) images reveal multilobular, CSF-filled, expanding spaces at the MDJ.

Perivascular spaces at the PMJ and MDJ among age subgroups

Age (y) Subgroup	Case (No.)	PVS at PMJ		PVS at MDJ	
		present	none	present	none
–20	12	11	1	9	3
21–40	42	35	7	24	18
41–60	34	31	3	26	8
61–	27	23	4	14	13
	total 115	100 (87%)	15 (13%)	73 (63%)	42 (37%)

Note.—PVS indicates perivascular spaces; PMJ, ponto–mesencephalic junction; MDJ, mesenecphalo–diencephalic junction.

Methods

Subjects

This study consisted of 115 adult subjects with ophthalmological complaints such as retro-orbital pain, double vision, and visual field defect without related pathologic findings at MR imaging. They underwent T2-weighted MR imaging in the past 4 years. The study population consisted of 65 men and 50 women, with a mean age of 45.6 years (range = 16–74 years).

The frequency and location of cystic lesions in the midbrain with signal intensity compatible to CSF were assessed on coronal, axial, and sagittal images. When present, the total number of high-signal-intensity spots and the maximum diameter of the largest one was graded on coronal images as follows: grade 0, less than 1 mm; grade 1, 1 mm or more and less than 2 mm; grade 2, 2 mm or more and less than 3 mm; grade 3, 3 mm or more and less than 4 mm; and grade 4, more than 4 mm and less than 5 mm. The diameters of the CSF hyperintensity were measured with calipers on the films and then graded by three of the authors (N.S., M.S., and Y.U.), and final decisions were made by consensus. The measurement in millimeters was obtained from the 1-mm reference scale found on each image.

Statistical Analysis

To explore the relationship between age and detectability of expanded PV spaces, subjects were classified into groups in increments of 20 years and detectability of PV spaces was assessed for each subgroup by the χ^2 test. A P value less than .05 was considered to be statistically significant.

MR Imaging

MR imaging was performed using a 1.5T system (Gyroscan ACS-NT; Philips, Best, the Netherlands) with a standard head coil. All images were obtained by a T2-weighted turbo spin-echo sequence with the following parameters: TR, 5800 ms; TE, 140 ms; FOV, 200 mm; section thickness, 3 mm; intersection gap, 0.5 mm; matrix, 284 × 512; echo train length, 23; and NEX, 4. To differentiate expanded PV spaces from lacunar infarcts, all subjects underwent T1-weighted MR imaging and proton density–weighted or fluid attenuated inversion recovery imaging. We counted only signal intensities compatible with those of CSF and a clear margin.

Histologic Studies

To evaluate expanded PV spaces histologically, two midbrain blocks from cadavers of 79- and 84-year-old women who died of non-neurologic causes were used. After fixation with 70% ethanol solution for 4 months, the midbrain was sectioned coronally for one specimen and axially for the other, into 3 mm-thick tissue blocks and embedded in paraffin. Sections (4 μm) were stained with hematoxylin and eosin and the Kluver-Barrera technique. The sections were viewed with low-powered light microscopy at magnifications of up to 50×.

Results

MR Imaging Study

In the lower midbrain, ovoid or linear spots with signal intensity compatible with CSF were present in 100 (87%) of 115 subjects (Table). Spots were most common between the cerebral peduncle and substantia nigra and occurred less frequently in the cerebral peduncle on axial sections (Figs 2 and 3). They were consistently located at the PMJ on coronal section. The number of spots per patient ranged from one to seven, with a mean of 2.3. Of the total number of the largest spots, 52% were assigned grade 0, 38% were assigned grade 1, 7% were assigned grade 2, 2% were assigned grade 3, and 1% were assigned grade 4 (Fig 2).

In the upper midbrain, round or ovoid CSF signal intensities were visible in 73 (63%) of 115 subjects (Table). They were distributed in the region of the MDJ. The number of spots per patient ranged from

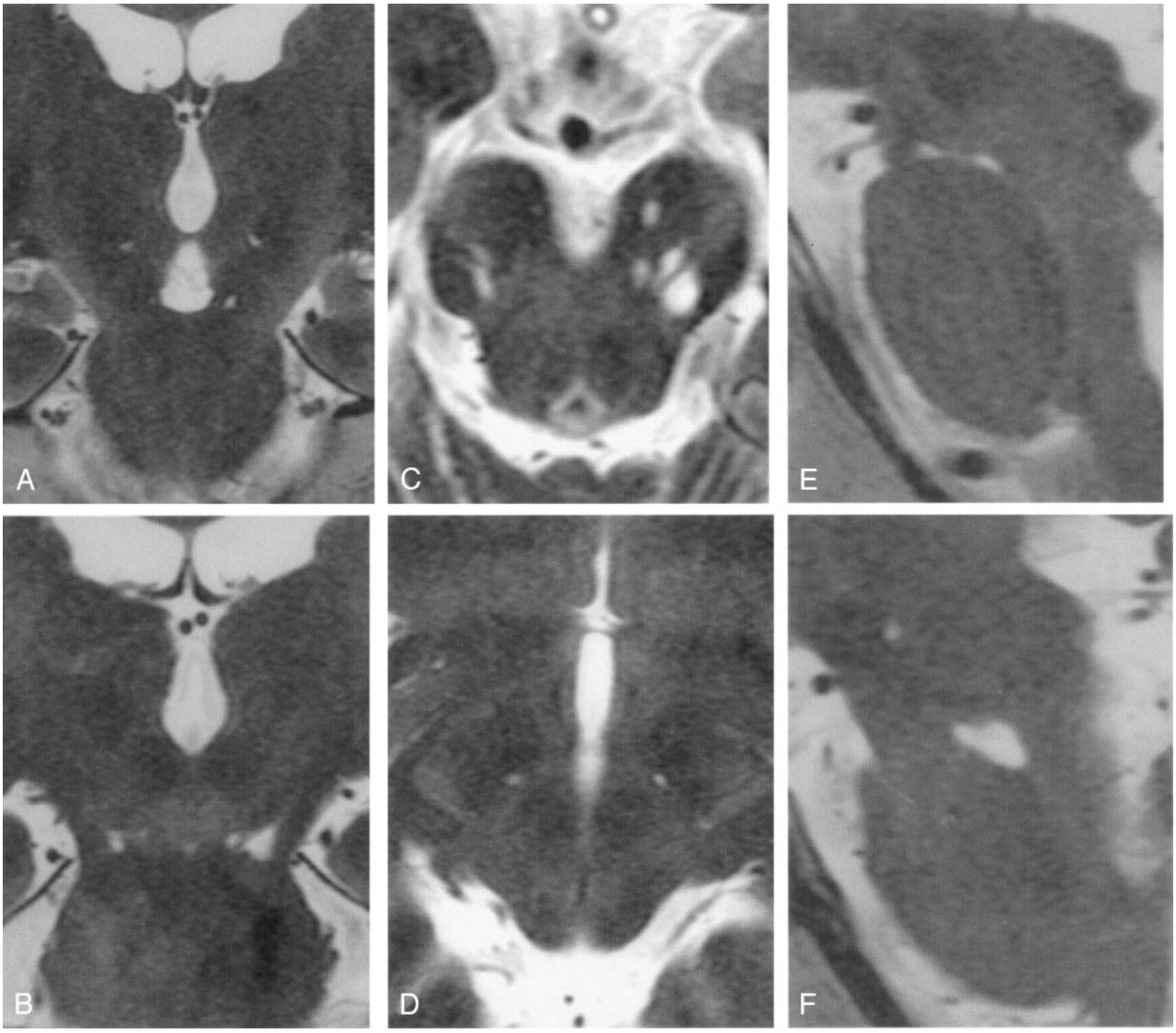

FIG 2. MR images obtained in a 48-year-old-man who presented with double vision due to the left nerve palsy.

A, Coronal section at the anterior midbrain. Expanded PV spaces are visible as round or ovoid hypointense lesions at the PMJ and the MDJ.

B, Coronal section at the cerebral peduncle. Expanded PV spaces are visible at the level of the PMJ, corresponding to the tentorial margin. The largest segment of the PV space is graded 4.

C, Axial section at the lower midbrain. Multiple ovoid and round PV spaces are visible between the cerebral peduncle and substantia nigra and in the cerebral peduncle.

D, Axial section, two sections rostral to Figure 2C. Small PV spaces are visible behind the cerebral peduncle.

E, Sagittal section, two sections lateral to the midline. Expanded PV spaces are visible between the pons and midbrain.

F, Axial section, four sections lateral to the midline. Large and small PV spaces are visible at the PMJ and MDJ.

one to 4, with a mean of 1.2. A total of 73% were grade 0, 23% were grade 1, 3% were grade 2, and 1% were grade 3. In both lower and upper midbrain sections, signal intensity abnormalities were located off the midline. In this study, the presence of PV spaces was not related to age for either lower ($P > .25$) or upper ($P > .1$) midbrain (Table).

Since our study was not prospectively designed and since complete images of the whole brain were not routinely obtained because of patients with ophthalmological complaints and signs, we did not attempt to correlate the presence of the midbrain PV spaces with those elsewhere in the brain. However, expanded PV spaces around the anterior commissure and basal ganglia were seen in association with those at the midbrain in several subjects; conversely several subjects had the midbrain lesions as an isolated finding.

Histologic Studies

Spaces lined with a pial layer and with an artery were revealed dorsal to the cerebral peduncle on axial and coronal sections at both the PMJ and MDJ (Fig 4). The presence of expanded PV spaces was confirmed histologically (1–6).

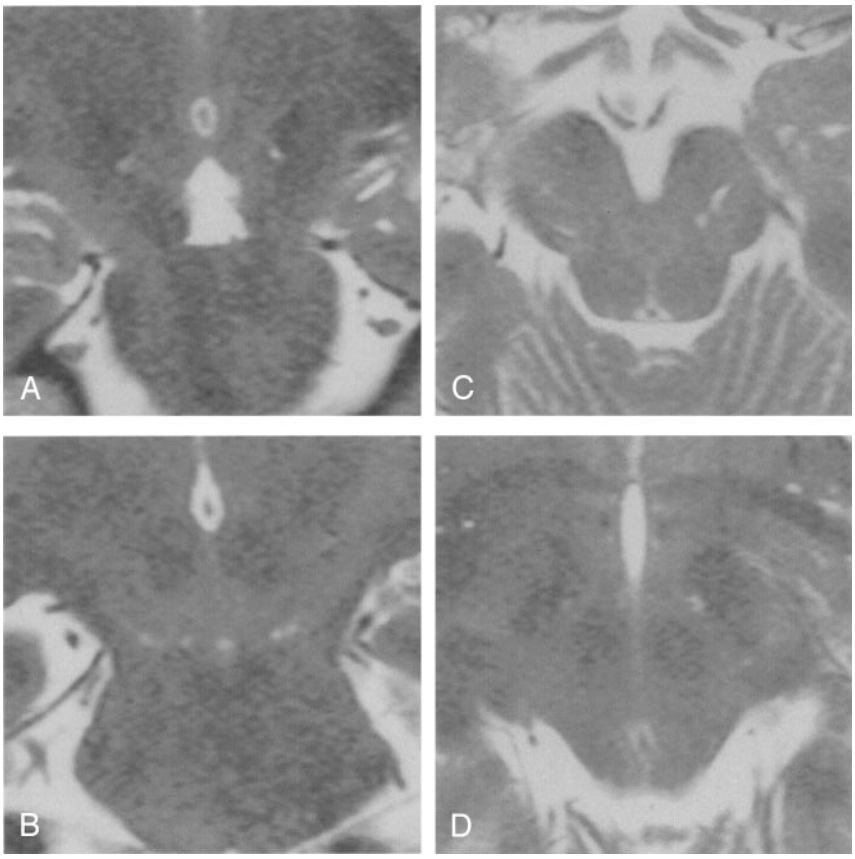

FIG 3. A 19-year-old female patient who complained of retro-orbital pain.

A, Coronal section at the cerebral peduncle. Round and ovoid PV spaces are visible at the level of the MDJ. The largest size is graded 1.

B, Coronal section two sections posterior to Figure 2A. Small PV spaces are visible at the PMJ and at the level of tentorial margin. The largest one is grade 0.

C, Axial section at the lower midbrain. Ovoid and linear PV spaces are visible between the cerebral peduncle and substantia nigra and in the cerebral peduncle.

D, Axial section, two sections rostral to Figure 3C. Small PV spaces are visible behind the cerebral peduncle.

Discussion

In 1991, Elster and Richardson (2) demonstrated PV spaces at the PMJ in 20% of normal subjects on MR imaging and histologic studies. Our findings, using heavily T2-weighted MR imaging, reveal that the incidence is as high as 87% at the PMJ. This higher rate of detection may be due to the MR imaging protocol, which is more sensitive for localizing CSF signal intensity (14). More importantly, expanded PV spaces are present in 63% of subjects at the MDJ at MR imaging and in two specimens studied histologically.

The MR imaging features of expanded PV spaces in the midbrain in the present study are similar to those reported by Elster and Richardson (2). At the PMJ, spaces are mainly located between the cerebral peduncle and substantia nigra in the axial plane and correspond to the level of the tentorial margin as seen in coronal sections. At the MDJ, although smaller and less conspicuous than those at the PMJ, they are located behind the cerebral peduncle on axial sections. To define PV spaces on MR images, their distribution needs to conform to the path of penetrating arteries (1–6). In the lower midbrain, enlarged PV spaces at the PMJ are routinely supplied by penetrating branches of the collicular and accessory collicular arteries (2, 15). In the upper midbrain, where the enlarged PV spaces are visible at the MDJ, they are supplied by the posterior (interpeduncular) thalamo-perforating artery or the paramedian mesencephalo-thalamic artery and short and long circumferential arteries originating from the upper basilar artery or proximal posterior cerebral artery (15, 16).

Expanded PV spaces in the midbrain have been reported in isolated cases. One case, reported by Romi (17), presented with Parkinsonism and the CSF signal intensity lesions were located at the PMJ. Kanamalla and colleagues (9) reported a case of mild ventricular enlargement and cavernous expansion of midbrain PV spaces. Follow-up MR imaging studies revealed no progression of enlargement in those cases. Such previously reported lesions may be similar to patients in our study who had PV spaces as large as 5 mm at the maximum and were free of clinical signs. Since high-spatial-resolution MR imaging studies may reveal such incidental findings, interpretation of the MR images needs to be judicious in relation to symptoms.

Clinical interest in expanded PV spaces at the midbrain originated when Poirier et al (7), in 1983, reported autopsy findings in hydrocephalus from aqueductal stenosis caused by expansive lacunae. The so-called "expansive lacunae" is equivalent to extremely expanded PV spaces, as they were pathologically lined by a single stratum of epithelium-like flat cells and contained a small artery or arteriole (7). They were situated at the MDJ in the territory of the paramedian mesencephalo-thalamic artery.

On reviewing clinical reports, seven cases can be found that required neurosurgical intervention owing to intraparechymal mass lesions, which were interpreted as expanding lacunae in the midbrain on the

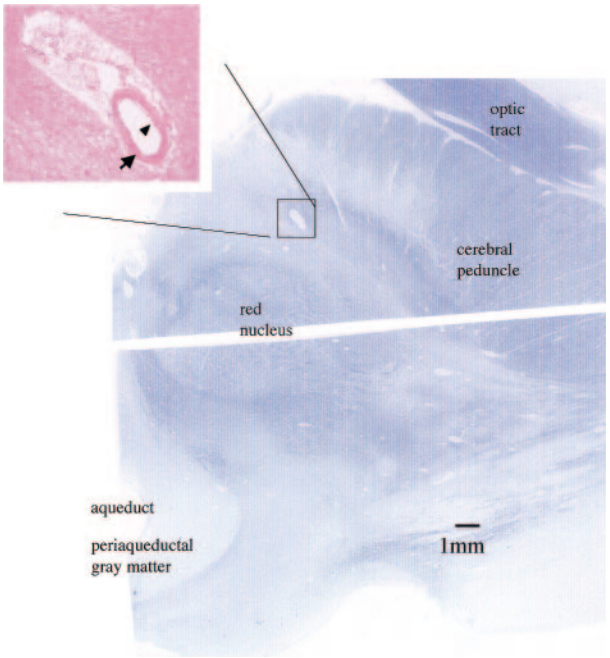

FIG 4. A, Axial section of the right upper midbrain. Kluver-Barrera stain (magnification ×4). Section line between ventral and dorsal halves is noted in the center. Aqueduct, periaqueductal gray matter, red nucleus, cerebral peduncle, and optic tract are demonstrated. Behind the cerebral peduncle, there is an ovoid space.

B, Magnified axial section demonstrating the PV space at the upper midbrain. H&E stain (magnification ×50). The ovoid space includes a vessel (*arrow*) and is lined by a pial layer (*arrowhead*). No necrotic or ischemic changes were visible in the surrounding brain tissue in this magnified view. Histologic findings histologically a PV space (1–5).

basis of specific MR imaging findings (8–13). All of them possessed the common MR imaging features of multilobulated cystic lesions with CSF signal intensity in the MDJ, which did not enhance. The predominant clinical manifestations were hydrocephalus due to aqueductal stenosis (six cases) accompanied by Parkinsonism (one case). Motor weakness was the main sign in the remaining case (12) (Fig. 1). All patients underwent VP shunt surgery or endoscopic third ventriculostomy (8–13). Surgical specimens obtained in three cases showed no epithelial lining, which might exclude cystic causes such as ependymal cyst or neuroepithelial cyst and might indirectly support the possibility that the cystic lesions originated from PV spaces (11–13). Recent reports suggest that PV spaces may cause a mass effect in the cerebral and cerebellar hemispheres (18, 19). Such pathologic and clinical evidence further confirms the presence of expanding PV spaces at the midbrain.

The mechanisms underlying expanding PV spaces are unknown. The autopsy study by Poirier et al (7) revealed segmental necrotizing angitis of the arteries, which, they speculated, caused abnormalities in the permeability of the arterial wall. The mechanism causing the angitis was unclear. Another possibility is that expanding PV spaces result from disturbance of drainage route of interstitial fluid due to CSF circulation in the cistern (8, 10). In the cervical spinal cord, it is hypothesized that nontraumatic obstruction of the CSF pathways in the spinal subarachnoid space results in cord enlargement with parenchymal T2 prolongation (20). These explanations on the change of brain and spinal cord are based on the speculation that the PV spaces are the outward route of interstitial fluid to and the inward route of the CSF from the subarachnoid space (8, 10). Either hypothesis is based on a pathologic modification of normal processes associated with PV spaces. We speculate this study supports the hypothesis that normal PV spaces at the MDJ undergo pathologic modifications and expand. The pathologic processes that affect PV spaces await future confirmation.

Clinically, expanding PV spaces with cystic components in the midbrain need to be differentiated from intraparenchymal lesions such as gliomas with cystic components, parasite infections, and other non-neoplastic intracranial cysts (ependymal, neuroepithelial, and arachnoid cysts) (10, 21). Those lesions may be differentiated on the basis of CT and MR imaging findings such as the presence of calcification, multilocular or monolocular shape, and signal intensity of cyst contents compatible with CSF (10). Since the therapeutic strategies depend upon the specific disease, precise diagnoses are important. Expanding PV spaces should be kept in mind as a differential diagnosis for intraparenchymal cystic lesions in the midbrain with signal intensity compatible with that of CSF.

Conclusion

This study revealed that expanded PV spaces were visible at the PMJ and MDJ. Our finding of expanded PV spaces normally present at the MDJ may be related to pathologically expanding PV spaces, which should be kept in mind as a differential diagnosis for intraparenchymal cystic lesions in the midbrain with signal intensity compatible with CSF.

References

1. Braffman BH, Zimmerman RA, Trojanowski JQ, et al. **Brain MR: Pathologic correlation with gross and histopathology. 1 lacunar infarction and Virchow-Robin spaces.** *AJR Am J Roentgenol* 1988;151:551–558
2. Elster Ad, Richardson DN. **Focal high signal on MR scans of the midbrain caused by enlarged perivascular spaces: MR-pathologic correlation.** AJNR *Am J Neuroradiol* 1991;11:1119–1122
3. Heier LA, Bauer CJ, Schwartz L. **Large Virchow-Robin spaces: MR-clinical correlation.** *AJNR Am J Neuroradiol* 1989;10:929–936
4. Jungreis CA, Kanal E, Hirsch WL, et al. **Normal perivascular spaces mimicking lacunar infarction: MR imaging.** *Radiology* 1988;169:101–104
5. Sasaki M, Sone M, Ehara S, Tamakawa Y. **Hippocampal sulcus remnant: potential cause of change in signal intensity in the hippocampus.** *Radiology* 1993;188:743–746
6. Song CJ, Kim JH, Kier EL, Bronen RA. **MR imaging and histologic features of subinsular bright spots on T2-weighted MR images: Virchow-Robin spaces of the extreme capsule and insular cortex.** *Radiology* 2000;214:671–677
7. Poirier J, Gaston BA, Meyrignac C. **Thalamic dementia. Expansive lacunae of the paramedian thalamo-mesencephalic territory.** Hydrocephalus caused by stenosis of the Sylvian aqueduct. *Rev. Neurol. (Paris)* 1983;139:349–358
8. Homeyer P, Cornu P, Lucette L, Chiras J, Derouesne C. **A special**

form of cerebral lacunae: expanding lacunae. *J Neurol Neurosurg Psychiatry* 1996;611:200–202.
9. Kanamalla US, Calabro F, Jinkins JR. **Cavernous dilatation of mesencephalic Virchow-Robin spaces with obstructive hydrocephalus.** *Neuroradiology* 2000;42:881–884
10. Mascalchi M, Salvi F, Godano U, et al. **Expanding lacunae causing triventricular hydrocephalus: Report of two cases.** *J Neurosurg* 1999;91:669–674
11. Ono Y, Suzuki M, Kayama T, Yoshimoto T. **Multilobulated cystic formation in the brain stem with Benedikt's syndrome: case report.** *Neurosurgery* 1994;34:726–729
12. Schroeder HWS, Gaab MR, Warzok RW. **Endoscopic treatment of an unusual multicystic lesion of the brain stem: case report.** *Br J Neurosurg* 1996;10:193–196
13. Wilkins RH, Burger PC. **Benign intraparenchymal brain cysts without an epithelial lining.** *J Neurosurg* 1998;68:378–382
14. Mamata Y, Muro I, Matsumae M, et al. **Magnetic resonance cisternography for visualization of intracisternal fine structures.** *J Neurosurg* 1998;88:670–678
15. Duvernoy HM. *Human Brainstem Vessels*. Berlin: Springer-Verlag, 1978;16–66
16. Saeki N, Rhoton AL, Jr. **Microsurgical anatomy of the upper basilar artery and the posterior circle of Willis.** *J Neurosurg* 1977;46:563–578
17. Romi F, Tysnes OB, Krakenes J, et al. **Cystic dilatation of Virchow-Robin spaces in the midbrain.** *Eur Neurol* 2002;47:186–188
18. Benhaiem-Sigaux N, Gray F, Gherardi R, et al. **Expanding cerebellar lacunaes due to dilatation of the perivascular space asociated with Binswanger's subcortical arteriosclerotic encephalopathy.** *Stroke* 1987;18:1087–1092
19. Davis GA, Fitt GJ, Kalnins RM, Mitchell LA. **Increased perivascular spaces mimicking frontal lobe tumor.** *J Neurosurg* 2002;97:723
20. Fischbein, NJ, Dillon WP, Cobbs C, Weinstein PH. **The "presyrinx" state: a reversible myelopathic condition that may precede syringomyelia.** *AJNR Am J Neuroradiology* 1999;20:7–20
21. Vanneste J, Hyman R. **Non-tumoral aqueductal stenosis and normal pressure hydrocephalus in the elderly.** *J Neurol Neurosurg Psychiatry* 1986;49:528–535